International Journal of
INTELLIGENT SYSTEMS AND APPLICATIONS IN ENGINEERING
ISSN:2147-6799 www.ijisae.org Original Research Paper

Design and Implementation of Brain Emotional Controller for Load Frequency Control in Multi-Area AGC

J. Shankar*[1], G. Mallesham[2]

Submitted:15/08/2025 **Revised:**25/09/2025 **Accepted:**08/10/2025

Abstract: An artificial intelligence controller called the Brain Emotional Learning Based Intelligent Controller (BELBIC) was inspired by the limbic systems of mammals. It has been used successfully in the field of control systems. This abstract presents simulation findings obtained using MATLAB/Simulink to analyze the performance of a power system exposed to shocks and parameter changes while accounting for the system's intrinsic nonlinearity. An automatic generation control (AGC) system was created by this work. The parameters of PI controllers are optimized using a range of readily available optimization techniques, such as Genetic Algorithm (GA) and Particle Swarm Optimization (PSO). The controller parameter (ITSE) is evaluated by each of these algorithms using a different cost function, such as the square error multiplied by integral time. By employing the computationally intelligent BELBIC technique, the performance of the AGC system was enhanced. Using readily available optimization approaches, the effectiveness of the GA-PI and PSO-PI controllers was compared with that of the BELBIC. The majority of the work currently in publication on AGC uses traditional methods for selecting the best controller parameters, such as Integral Time Squared Error (ITSE). This problem is addressed by the proposed BELBIC. The simulation results demonstrate the BELBIC's dependability and sensitivity to changes in parameters and load. It outperforms the GA-PI and PSO-PI controllers under a range of operational load scenarios, particularly when it comes to managing the load frequency tuning problem in multi-area power plants. The results demonstrate the BELBIC's efficacy as a power system control solution.

Keywords: *Load frequency control (LFC), Brain emotional learning based intelligent controller (BELBIC), Automatic generation control (AGC), Genetic Algorithm (GA), Particle Swarm Optimization (PSO).*

1. Introduction

The growing population and rising demand for electricity in the modern world make it impossible for conventional energy sources to meet the demand. Tie lines are consequently required in order to address this problem by establishing a connection between several separate conventional sources. Their connectivity allowed the loads to be distributed across the numerous sources and readily withstand power system disturbances. Although connecting across different places is more likely to be advantageous, the frequency of the system is affected by load variance. Any variation in the load during operation, for whatever reason, only affects the frequency of that energy source. However, when many energy sources are operating, any changes in load in any part of the power system affect both the frequency and the power transferred across the tie line. Because the main controller previously depended on the governor's action to restore the system's operating frequency to its pre-disturbance value, there is still a steady state frequency inaccuracy. Consequently, the steady-state error is eliminated and the system's order is increased by using a second controller. This controller is referred to as a secondary or integrated controller. Since LFC offers electricity in a more reliable and improved form, it is essential for the power system to function and be managed efficiently.

Maintaining the appropriate capacity for the frequency, voltage profile, and load flow conditions is the primary goal of an electrical power system. Demand and power generation must be balanced in order to deliver reliable, high-quality power generation to consumers. While maintaining the system frequency and interchanged power at the predetermined levels, a limited number of control areas or regions operating in grid-connected mode are able to provide enough electricity to satisfy the customers' load requirements. In order to guarantee that the electricity supplied meets the required quality requirements, Automatic Generation Control (AGC), also known as a load frequency controller [1-2], is designed and put into use to automatically balance generated power and load demand in each control region. LFC's primary goal is to return the system's tie line power and frequency to their baseline levels prior to the disturbance. It will be beneficial to control the generating units' usable power in order to achieve this [3–4]. Everyone is aware that the load fluctuates constantly throughout the day. The stored kinetic energy in the generator prime mover set adjusts the load demand in a steady-state power system, resulting in a commensurate shift in frequency and speed [5-7].

There, various methods for resolving the AGC problem have been examined. For the electrical system to operate safely, load frequency management is therefore essential [8–9]. One of LFC's

1 Department of Electrical Engineering, University College of Engineering, Osmania University, Hyderabad ORCID ID : 0009-0005-7227-3643

2 Department of Electrical Engineering, University College of Engineering, Osmania University, Hyderabad ORCID ID : 0000-0001-7100-6256

** Corresponding Author Email: drjsr@osmania.ac.in*

main objectives is to return the system tie line power and frequency to their baseline levels prior to the disruption. It covers both single- and multi-area power systems that fall into these two categories; hence, controlling the generating units' usable power would be beneficial [10–11]. A power system should be controlled and limited to a certain level of variation [12–13]. Among these tactics are PID controllers combined with optimisation techniques and soft computing. have been created to improve transient responsiveness through load frequency management and automatic generation control (AGC) research [14–15]. Swarm intelligence is the collective behaviour of self-organising, unstructured systems [16]. Swarm intelligence is the collective behaviour of self-organised and unstructured systems [17–19]. Genetic algorithms (GAs) are used to optimise a proportional integral (PI) controller for frequency management in an AGC-Multi Area structure that is prone to load fluctuations and other abnormalities [20–21]. Based on swarm intelligence, a variety of artificial algorithms have been developed to address optimisation challenges. Models are built utilising a linear method in order to reduce framework and analytical techniques [22]. Under the assumption that the wind speed stays constant, a transfer function model is developed for the wind power plant, which has a nominal rating of 35 MW and is further connected to the two Area Networks. The reheat thermal structure of the system was developed considering both reheat thermal constraints and generating rate constraints. An overview of the implementation of this technique is given in the following procedure [23].

In this study, we propose the brain emotional controller to overcome the shortcomings of the existing controllers. A technique for managing intricate nonlinear situations, the brain emotional controller is presented by Caro Lucas [24–25]. BELBIC is a model-free, direct adaptive controller with a straightforward structure, quick autolearning, and little online computation. Its proper learning ability makes it robust to parameter alterations and extremely powerful in handling disturbances. The controller's model is known as the "centre of emotions" because it incorporates elements of the Limbic system that are present in the human brain. The brain emotional controller is used in many industrial products, including washing machines, cranes, and air conditioners, based on emotional learning in the human brain, a self-tuning load frequency control method for microgrids has been developed [26-29]. For an AVR system in power systems, an effective optimal fractional emotional intelligent controller has been presented. [31] The brain's emotional controller architecture, which integrates reward and sensory functions, is essential for the development of both sensory and emotional signals. The plant output, the error signal, and the controller output are all inputs to the controller. The functional sensory signal that the controller's input is converted into is then further processed to produce an emotional response signal. To maximise the controller's and the system's variable parameters' gains, computational optimisation techniques are employed. The convergence, accuracy, and robustness of these methods influence their effectiveness.

2. Mathematical Modeling Of The Three Area System

The system's thermal, wind, and hydroelectric components can generate 2000 Mw, 35 Mw, and 2000 Mw of power, respectively. These facilities share power via a tie line [31–32]. The producing rate and reheat restrictions were taken into account when developing the thermal system model [33–34]. It has long been believed that wind farms run at a steady pace. Each system has three different PI controllers. For each of the three plants, transfer function models have been created for frequency response analysis. Models are developed in a linear approach to minimise model and analysis processes [35]. A wind power plant with a nominal rating of 35 Mw is further connected to the two-area network, and a transfer function model for the wind power plant is developed assuming a constant wind speed [36]. The three power systems' MATLAB/SIMULINK connections are shown in Fig. 4. Several features of a thermal-wind-hydro power system with a BELBIC, GA-PI, and PSO-PI controller are shown in Tables 1 through 4 The Wind Energy Conversion System's (WECS) dynamic performance can be described using the two-pole-one-zero transfer function below. The hydro unit is shown in Figure 2, the generic speed controlling system model is shown in Figure 1, and Figure 3

Table:1 The parameters of the simulated system

The modeled reheat thermal and hydro power plant's descriptive specifications	
P_r	2000Mw
K_r	0.5
T_g	0.08sec
T_t	0.3sec
f	50Hz
K_p	120Hz/p. u Mw
T_r	10sec
$P_{tie\ max}$	200Mw
T_p	20sec
H	5 sec
P_r	35 Mw
D	0.00833 p.u. Mw/Hz
R	2.4 Hz/p.u. Mw
Specifications for Parametric analysis Wind Power Plant Simulation	
Air Density	1.2 kg/m^3
Gear ratio	70
T_{pt}	10.55
Turbine blade radius	45m
K_{pt}	0.012
H	5 sec
The mean wind speed	7m/s
T_i	3 sec
T_p	20 sec
T_{12}	0.544

2.1. REHEAT THERMAL UNIT

In large-scale power plants, reheat thermal generation power systems with speed controlling systems are a popular form of power generation system. It effectively produces electricity by fusing the ideas of a reheat thermal cycle with a speed-governing system. By adjusting power supply to demand, the speed regulation system also helps to maintain grid stability. Warm up the thermal areas that were inspected. An equal single-area power system consists of a steam turbine with a reheater and a governor. The transfer function of the governor is shown in equation (1). The dynamic model of the Reheat thermal area is shown in Fig. 1.

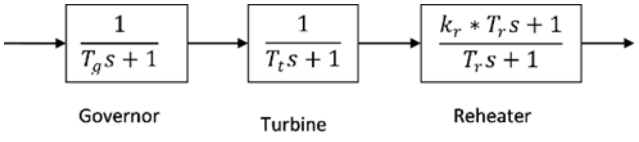

Fig.1 Reheat Thermal Unit

$$G_{gt}(s) = \frac{K_g}{T_g.s + 1} \quad (1)$$

The pressurised steam that enters through a steam inlet valve causes the turbine to expand. Equation (2) provides an expression for the transfer function of the steam turbine.

$$G_{Tt}(s) = \frac{K_t}{T_t.s + 1} \quad (2)$$

The expansion of steam inside a turbine results in steam exhaustion and a rise in moisture content. Therefore, the steam generated by the steam turbine must be heated once again to eliminate any residual moisture. Equation (3) can be used to characterise the transfer function of a typical re-heater.

$$G_{Rh}(s) = \frac{K_r.T_r.s + 1}{T_r.s + 1} \quad (3)$$

2.2. HYDRO POWER STATION

In hydroelectric power plants, an electric governor in conjunction with hydro turbine power generation usually regulates the turbine generator's speed and power production. It blends an electronically controlled regulating mechanism with the fundamentals of hydraulic power generation. An essential part of hydroelectric power facilities, the electric governor system guarantees optimal turbine performance, grid stability, and the capacity to adapt to fluctuating load needs. The hydro components of the power system that are being studied, which include the electric governor and hydro turbine, are equivalent. The dynamic model for the hydro areas is shown in Fig. 2.

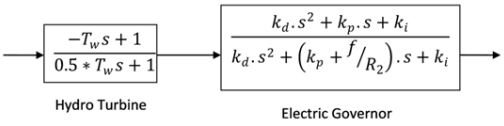

Fig.2 Hydro Unit

The hydraulic turbine's transfer function (T/F) is,

$$G_{Ht}(s) = \frac{-T_w.s + 1}{0.5T_w.s + 1} \quad (4)$$

The hydraulic governor's transfer function (T/F) is

$$\frac{K_d.s^2 + K_p.s + K_i}{K_d.s^2 + \left(K_p + \frac{f}{R_2}\right)s + K_i} \quad (5)$$

2.3. WIND ENERGY CONVERSION SYSTEM

The two-pole-one-zero transfer function shown below can be used to describe the dynamic performance of the Wind Energy Conversion System (WECS): The transfer function determines the intrinsic frequencies and damping ratios of the Wind Energy Conversion System (WECS). It introduces novel dynamics that impact the behaviour of the system, such as oscillations, settling time, and overshoot. The parasitic time constant is Tϵ, and the primary time constant is Tpt. The second-order dynamics of the wind energy conversion system can be derived by choosing the right natural frequency ωn and damping factor γ, which then yields the controller settings. The closed loop architecture of WECS under PI control is shown in Figure 3.

$$T_i = \frac{2\gamma}{\omega_n} - \frac{1}{\omega_n^2 T_{pt}} \quad (6)$$

$$K_p = \left(\frac{T_i T_p}{K_{pt}}\right) \quad (7)$$

$$H_{pt}(s) = \frac{K_{pt}(T_{zs} + 1)}{(T_{\varepsilon s} + 1)(T_{pt} + 1)} \quad (8)$$

T_{pt}, T_{ε} are the main and parasitic time constant

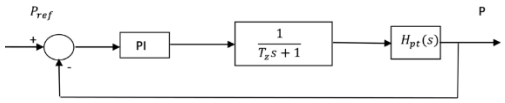

Fig.3 Wind Energy Conversion system

The Integral Time Square Error (ITSE) was chosen as the performance index, which can be written as:

$$ITSE = \int t.\left\{(\Delta f_i)^2 + \left(\Delta P_{tie_{i-j}}\right)^2\right\} dt. \quad (9)$$

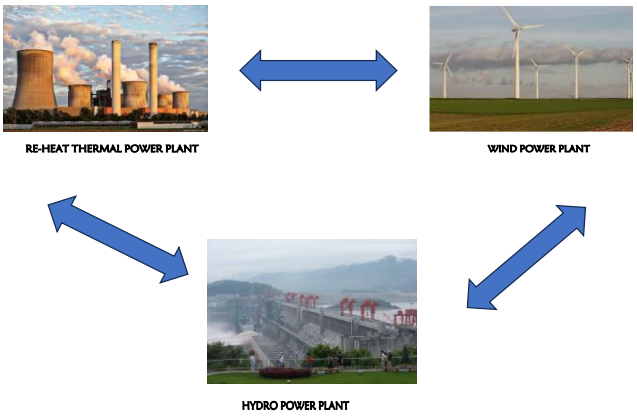

Fig.4 A graphical representation of three distinct yet linked regions via a tie-line

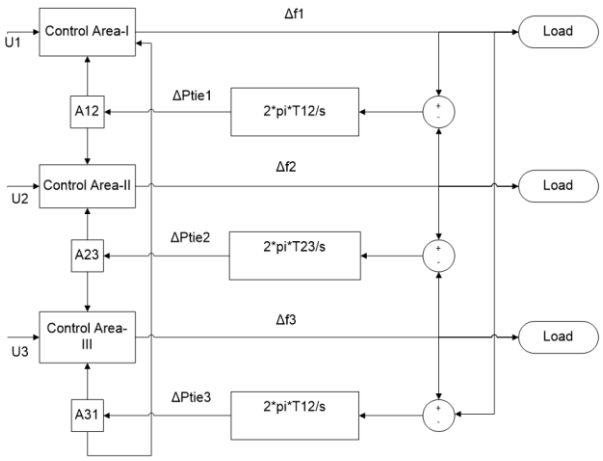

Fig.5 Block diagram Representation of interconnected of three area system

3. Control Techniques

3.1. PROPORTIONAL INTEGRAL (PI) CONTROLLER

In the limit of minute variations in the rate of controller output with minute variations in error, this mode is a logical progression of the floating control concept. Another name for this mode is reset action. Bit by bit, the erroneous signal must be integrated. The inaccuracy and the corrective signal's rate of change are strongly related. This controller's transfer function is

$$H(s) = \frac{U(s)}{E(s)} = K_p + {K_i}/{s} \quad (10)$$

The time domain model of the PI controller is also seen in Eqn (11). where e(t) provides the error-caused answer, u(t).

$$U(t) = K_p + K_i \int e(t)dt \quad (11)$$

MATLAB Simulink is used to generate the transfer function model for this controller, which is then used for load frequency regulation.

3.2. GENETIC ALGORITHM (GA)

In 1975, Holland developed the Genetic Algorithm (GA), a computational depiction of natural evolution, to address specific optimisation problems. It is a recurring search procedure that operates with a group of strings called chromosomes. An overview of the implementation of this technique is given in the following procedure [37–38]. GA solves optimisation issues by using random search. When searching a large space, GA may offer several benefits over traditional optimisation techniques. In this case, GA optimises the gains of the conventional PI controller performance index as fitness functions. The main issue when employing an optimal PI controller for frequency regulation of an AGC system is tuning the ideal values to solve by GA using an objective function (9). The PI-tuned GA controller is automatically established with goal functions and its performance is computed using time-domain boundaries on the closed loop response. A GA has enhanced the look of the computer system and operates without detail. It depends on how evolutionary operators like reproduction, cross-over, and mutation react. Analysing and starting the problem by population, development, exercise measurement, population fitness selection, and reproduction inside a GA yields the optimal solution fitness. *Reproduction:* creates a new generation of chromosomes; fitness proportionate reproduction is encouraged by roulette wheel selection. *Crossover:* enables information sharing among members of the population. Following the random selection of two parent strings, a new child string is created by combining a random substring from the parent strings. *Mutation:* random alteration of a string's bits that results in a bit changing from 1 to 0 or vice versa. A new generation is created once the mutation process is complete, and the process is repeated to evaluate the new fitness. Set up the population's chromosomal strings. Find the strings and evaluate them. Select the fitness strings. Paste the best strings on to the ones that were not chosen. Create off strings by combining and developing it. Stop the process and update the genetic cycle

3.3. PARTICLE SWARM OPTIMIZATION (PSO)

Similar to other evolutionary computation methods, particle swarm optimisation starts with an initial population of individuals and looks for optima. The members of this initial population are then updated and relocated to a better location utilising some kind of process. Four well-known evolutionary algorithms—genetically, evolutionary programming, genetic algorithms, and genetic algorithms—were inspired by evolutionary events found in nature. They then appropriate the concepts of evolution of the fittest and competitiveness. However, social behaviour simulation is the source of PSO's motivation. The concepts of individual competition and collaboration serve as its inspiration.

This approach is better than genetic and evolutionary algorithms in a few respects, though. First, PSO has memory. Stated differently, every particle has memory for both its ideal solution (local best) and the collective optimal solution (global best). Another advantage of PSO is that it keeps its original population, thus there's no need to add operators to it. Significant amounts of time and memory storage are needed for this process. To get the results in Table 2, the PSO uses a stochastic search technique enhanced by swarm intelligence. Because of this, PSO operates as an algorithm that makes use of collective intelligence. Numerous alternative solutions that were produced at random are included in this attempt. A swarm is made up of all of these potential solutions, each of which is referred to as a particle.

Every individual in the PSO system modifies their flying in a multi-dimensional search space based on their own and their companions' flying experiences. Every person is called a "particle," which stands for a potential fix for the issue. When the number of iterations increases by one, the coordinates of location (x) and velocity (v) align. Every particle in a D-dimensional space is regarded as a point. The ith particle is represented as X_i^k is ($x_{i1}^k\ x_{i2}^k\ x_{i3}^k \dots\dots x_{iD}^k$)T For a particle, the rate of position change (velocity) g is expressed as V_i^k is ($v_{i1}^k\ v_{i2}^k\ v_{i3}^k \dots\dots v_{iD}^k$)T indicates its current movement decision. Any particle's best prior location, which provides the highest fitness value, is noted and shown as P_i^k ($p_{i1}^k\ p_{i2}^k\ p_{i3}^k \dots\dots p_{iD}^k$)T is Among all the particles in the population, the best particle's index is shown. Eqn (12) describes a velocity update equation that modifies the i th particle's velocity.

3.3.1. Equation for updating velocity

In Particle Swarm Optimization (PSO), each particle's velocity is modified using the velocity update equation, which also refreshes their locations in the search space. This equation integrates social and cognitive elements to balance exploration and exploitation during the optimization process. The standard velocity update equation is as follows:

$$V_i^{k+1} = wv_{iD}^k + c_1 * r_1\left(P_{iD}^k - X_{iD}^k\right) + c_2 * r_2\left(P_{gD}^k - X_{iD}^k\right) \quad (12)$$

3.3.2. Equation for Position Update

In Particle Swarm Optimization (PSO), each particle's position within the swarm is adjusted based on its updated velocity using the position update equation.

$$V_{iD}^{k+1} = X_{iD}^k + V_{iD}^{k+1} \quad (13)$$

The particle index is denoted by i = 1, 2……, while dimensions are represented by D = 1, 2……. The letter S stands for the swarm size, while the acceleration constants for the social and cognitive scaling aspects are C1 and C2, respectively. Both r1 and r2 have uniformly distributed, randomly distributed integers between 0 and 1. (12) and (13), for example, show that the dimensions of each particle are changed independently. The aim function only links the issue space dimensions to the best-found gbest and pbest. Algebras (12)

and (13) define the PSO algorithm.

3.4. BRAIN EMOTIONAL CONTROLLER (BEC) SYSTEM ARCHITECTURE

Using a structural model for control engineering and decision-making that is based on the limbic system of the mammalian brain is the main goal of this study. This study is motivated by the effectiveness of functional emotion modelling in control engineering applications [39]. In order to simulate the amygdala, orbitofrontal cortex, thalamus, sensory input cortex, and other brain regions thought to be essential for processing emotions, we have embraced a network model created by Moren and Balkenius [40]. There are two possible perspectives on intelligent and cognitive control. The indirect method modifies the controller's parameters by means of the intelligent system. In our example, the BELBIC computational model, we choose the second, so-called direct approach, in which the intelligent system is represented by the controller block [41–42]. BELBIC is essentially a system that generates activities in reaction to sensory and emotional inputs. Due to the emotional reaction to the real activity of the mammalian brain, the emotional intelligent controller of the bio-inspired brain is very similar to the structure of the mammalian brain [43–45]. The limbic system, which includes the thalamus, amygdala, orbitofrontal cortex, and sensory cortex, is responsible for producing emotions. Unlike traditional controls, intelligent emotional reaction speeds up decision-making. All information sent to and from the cortex is processed by the thalamus, a part of the brain that also receives and interprets sensory data. It is essential for emotions, memory, and attention. It's possible that the thalamus filters or reduces noise in sensory feedback signals insufficiently. The sensory cortex inputs needed for differentiation and subdividing are set up by this thalamic region. Moren and Balkenius created a computer network model to construct the limbic system, which is made up of the amygdala (A) and orbitofrontal cortex (OFC) [46].

The almond-shaped amygdala in the brain is made up of two amygdales located in the hippocampus, which is in the front of the temporal lobe. Amygdale is essential for learning, memory, and a range of emotions. Specifically, during the decision-making phase of the interaction with the amygdala, the orbital cortex plays a major role in the production of fear and apprehension. Fig. 6 shows a model depiction. In reaction to sensory information and emotional cues, a process known as BELBIC generates actions. The sensory cortex, the outermost layer of the brain that receives input, is composed of two sensory cortexes: the main sensory cortex and the secondary sensory cortex. The primary sensory cortex detects muscle impulses and halts the processing of neural data. The information must be delivered to the secondary sensory cortex and registered in the location where the action is to be executed. The BEIC process is shown in Figure 5. The mechanism is at the heart of this. Two sensory inputs, Si and i = 1...n, and one output make up the proposed controller. According to Fig. 7, the brain's intelligent emotional controller has two states for each sensory input (Si): one linked to the amygdala output (Ai) and the other to the orbitofrontal cortex output (OFCi). The sensory signal (Si) is known to be a function, f. It consists of the following controller output (YC), plant output (YP), and error (e) representations:

The user must run the installation function included in the BELBIC toolbox file package from within the MATLAB R command line environment. To accomplish this, simply type >>install me at the command prompt. The MATLAB R application will automatically restart if the user selects the BELBIC toolbox.slx file during the installation process. The user can browse the newly installed Simulink R toolbox after the installation process is complete. As seen in Fig. 8, this toolbox is separated into four distinct axes. The user can locate some BEL primitive functions, including the thalamus and sensory cortex, in the common part. Both the continuous-time and discrete-time BEL formulations in the continuous-time and BEL systems share such objects.

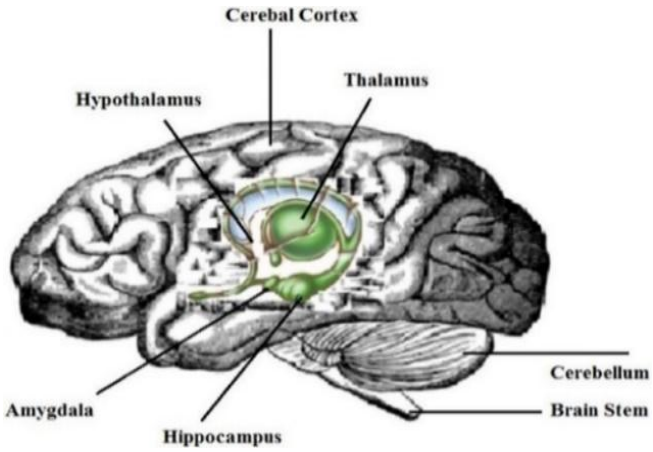

Fig. 6. Parts of the BELBIC

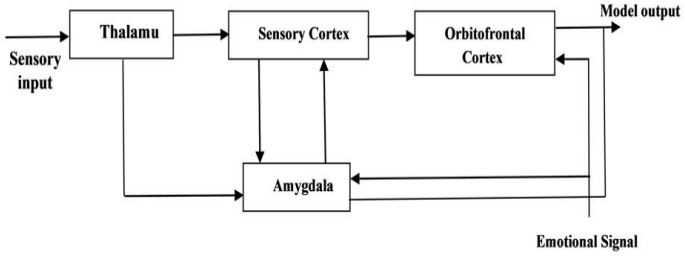

Fig.7 Intelligent Controller Model Based on Brain-Emotional Learning

Each of these components has a mask that is used to adjust it by establishing suitable initial conditions and learning coefficient values. Regarding the discrete-time version, the same is true. But in this instance, defining a sampling time is necessary for all the components. A collection of illustrative examples on how to effectively utilise the potential of the models that are offered may be found in the fourth sub-library. Some more complex control-based instances are given in addition to the most basic ones. Specifically, Mehrabian and Lucas's management of a non-linear continuous stirred tank reactor (CSTR). The toolbox contains information about the model and BEL controller parameterisation.

$$S_i = f(e) \tag{14}$$

$$f = K_1 e + K_2 \int e.dt \tag{15}$$

where K_1 and K_2, which are tuned in the experimentation premise, are the sensory gains in eq.15. The sensory cortex (SC_i) receives the sensory signal S_i eq.14, while the amygdala is only the thalamus's output.

$$SC_i = g(S_i) \tag{16}$$

$$g(S_i) = e^{s_i} \tag{17}$$

A_i and O_i, outputs are given by eq.18 and eq.20

$$A_i = V_i S_i \tag{18}$$

$$\Delta V_i = \propto (S_i \max(0, Rew - \sum_i A_i)) \tag{19}$$

where V_i eq.19 is the gain of A_i The output of the orbitofrontal cortex is expressed in eq.20

$$O_i = W_i S_i \tag{20}$$

where W_i eq.21 represents O_i gain. The A_i and O_i The internal weight update is passed through in the learning process.

$$\Delta W_i = \beta(S_i\,(E^i - Rew)) \tag{21}$$

The Δ symbol above denotes the weight differences. For Ai and Oi, the learning rates are α and β. With function J, the reward signal could be managed to obtain. Function J can be used to derive the reward signal in eq.23

$$\text{Reward Signal (REW)} = (e, y_p, y_c) \tag{22}$$

$$J = k_3(e \times y_c) + k_4(y_p) \tag{23}$$

Reward signal has K_3 and K_4 gains. The emotional signal output, E^i is achieved by combining the excitatory nodal output of the Amygdala with the inhibitory Orbitofrontal Cortex. The emotional signal output is produced by combining the excitatory Amygdala nodal and Orbitofrontal Cortex outputs, as seen below, E^i in eq.24

$$E^i = A_i - O_i \tag{24}$$

As a whole, the modified reward signal is expressed as

$$E = A - O \tag{25}$$

E is the ensuing emotional signal eq.25 at the controller. where K1, K2, K3, and K4 indicate the gains that must be changed to provide a good controller, ACE stands for area control error, and Δfi indicates the variation in frequency inside the area. The gain K1 can be used to modify the overrun. The gain K2 controls the adjustment of the settling time. Gain K3 calibrates the steady-state error, while gain K4 smoothes the earliest stages of the response. The controller's architecture activates the sensory signal function (Si) initially. The signal is processed by the thalamus before being sent to the sensory cortex and amygdala. The sensory cortex (SC) analyses the sensory signal. The SC speeds up the controller's response by producing the necessary signal and transmitting it to the orbitofrontal cortex (OFC) and amygdala (A). Selecting the right emotional cue strengthens the signal link between the OFC and the amygdala, allowing the signal to reach both A and OFC. He created the Amygdala. Emotional cues and learning rates are indicators of amygdala growth. The learning equation's max term makes the amygdala's output consistently high. By using the Orbitofrontal cortex (OFC) learning paradigm, the amygdala's response was rectified. Learning rate, EC, and SC are combined to create an orbitofrontal cortex (OFC) gain. If the plant's necessary response is met by the emotional signal that emerges from the interaction of the orbitofrontal cortex (OFC) and the amygdala (A) impulses in E, the process is over; if not, it begins anew.

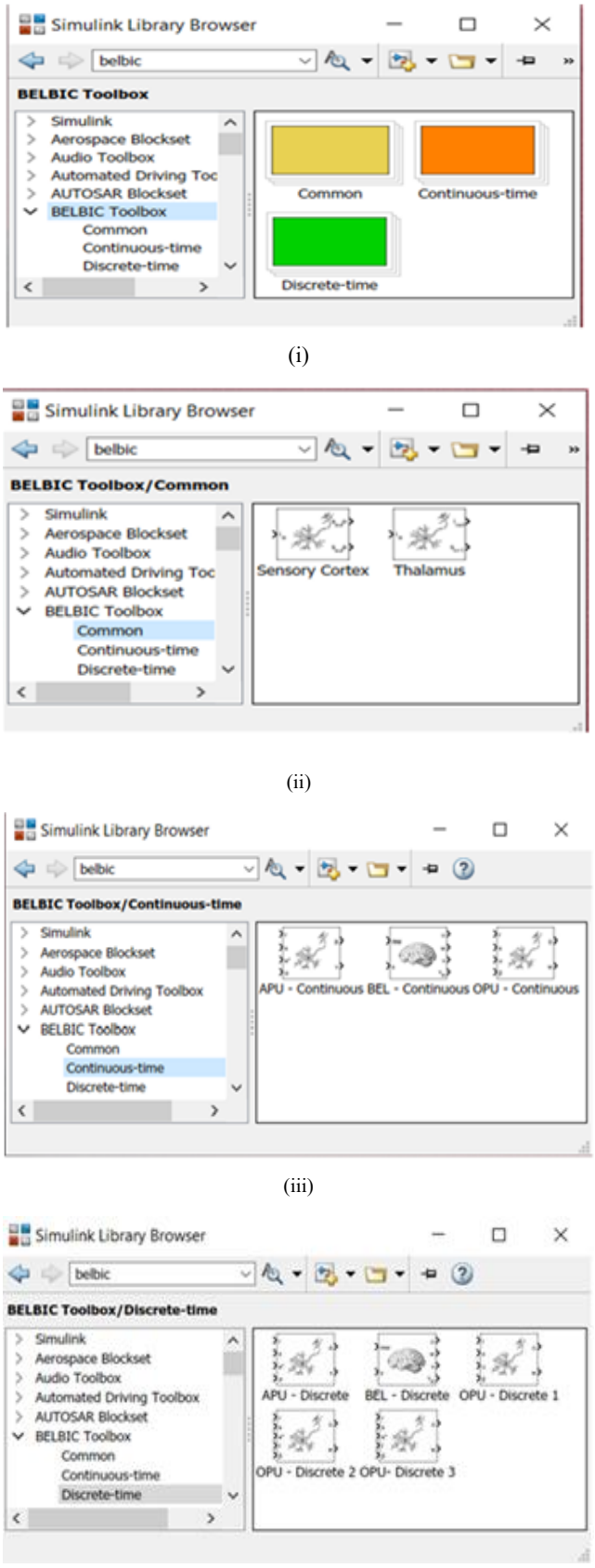

Fig.8 The BELBIC Simulink Tool box structure

4. Simulation Results And Discussion

The suggested power system model consists of three interrelated regions: reheat thermal, hydro, and wind zones. The appendix contains the system's parameters. The proposed model has a controller in each section. The BELBIC, GA-PI, and PSO-PI controllers were all covered in this study. Last but not least, there are nine gains: V, Vth, and W are the beginning circumstances of each region's orbitofrontal cortex (OFC) and amygdala output, which are likewise adjusted by the BELBIC's emotional approach. The regions of the brain with gain values include K1, K2, for sensory input, K3, K4, for reward signal, and α and β. In each of the three domains, the BELBIC and MATLAB/Simulink are used to simulate the proposed model.

Frequency Responses To demonstrate the improvements, one area (Area 1) is chosen for each model, and the frequency response (bold line) of the BELBIC, PSO-PI, and GA-PI controllers is shown in the table. The GA optimised PI controller deviates less from the nominal frequency value (50 Hz), as seen in Figures 9, 11, and 13. The frequency of the system stabilises after 1%, 2%, and 5% load disturbances, although the default GA-PI and PSO-PI controller shows more pronounced undershoot and overshoot steady-state error and settling time to its frequency characteristics. Furthermore, it stabilises much more slowly than the BELBI Controller.

Tie-line Control the BELBI Controller affected the system when we looked at the tie-line power exchange between regions 1 and 3. It illustrates how the modified controller improved the overshoot and undershoot characteristics of the tie-line power exchange signal and dramatically decreased the early oscillations. The interchange between areas concluded much earlier, even if the default GA-PI and PSO-PI controller did not perform well in all of the signal characteristics mentioned above. When tuned with the proposed BELBIC, the model's controller showed much less improvement in initial oscillations than the default GA-PI and PSO-PI controller. However, the signal's characteristic was almost entirely removed in a shorter period of time to halt the tie-line power exchange between areas 1 and 3. You may see this in Fig.9, 11 and 13. The MATLAB/Simulink platform was used to design and construct a multi-area reheat power system, which was the subject of this paper. To assess the enhanced performance of the suggested method, the necessary power system is simulated using a BELBI controller and step load perturbations (SLPs) of 1%, 2%, and 5% in Area 1.

4.1. SECTION-1

The proposed model is simulated in MATLAB/Simulink under a 0.01 p.u. change in load demand in Area-1 using the recommended controller BELBIC. For the system dynamic reactions, Figs. 9 and 10 display the frequency fluctuations, Tie-line power variations, and Area Control Error fluctuations of the Reheat thermal area, wind area, and hydropower region, respectively. The BELBIC has better peak overshoot and peak undershoot characteristics and settles faster, despite having a faster settling time than the PSO and GA tuned controller. Accordingly, the measured system response, frequency deviation, tie-line power flow, and area control error variations are shown for the closed-loop system in Figs. 9 and 10. The following Table.2 describes the gains made by the controllers. In the end, the developed controller exhibits superior dynamic responsiveness. In comparison to the other locations, it has the least amount of overshoot peak. In comparison to the other areas of the values, Area-1 displays a positive overshoot peak with regard to the tie-line power flow. As a result, the recommended BELBIC controller outperforms the GA-PI and PSO-PI controllers for the Multi Area Power System. The controllers' gains are summarised in Table 2.

It demonstrates how well the BELBIC controller reduces frequency and tie-line power variations. The dynamic frequency and tie-line power responses are shown in Figures 9–10, and the area control error findings obtained clearly show how well the BELBIC controller works to reduce emerging frequency and tie-line power deviations. Figures 9–10 display the frequency, tie-line power, and area control error responses of the power system with BELBIC adjusted using a hit-and-trial approach. When compared to GA-PI and PSO-PI that are adjusted through trial and error, BELBIC significantly reduces peak overshoot and undershoot, and frequency deviations rapidly settle down to zero values. Table 2 shows the results in terms of peak overshoot and settling time.

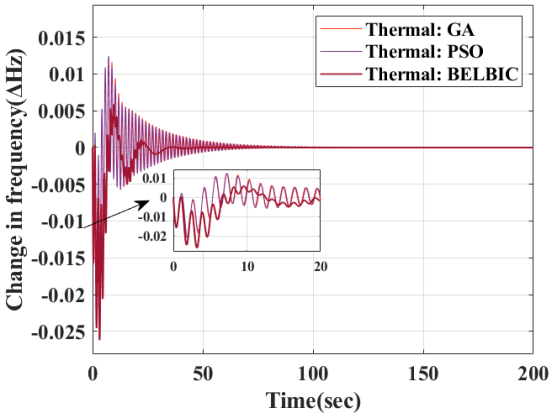

(i)

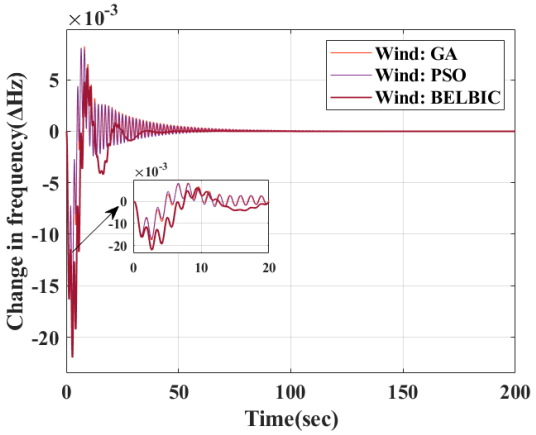

(ii)

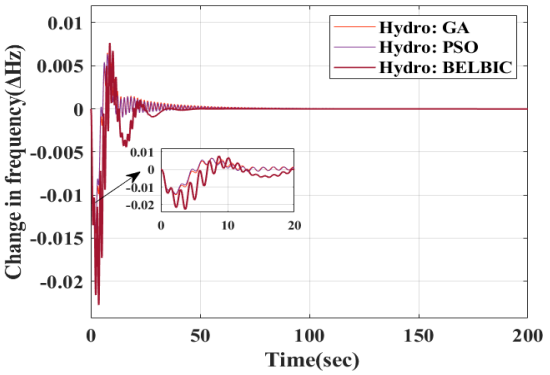

(iii)

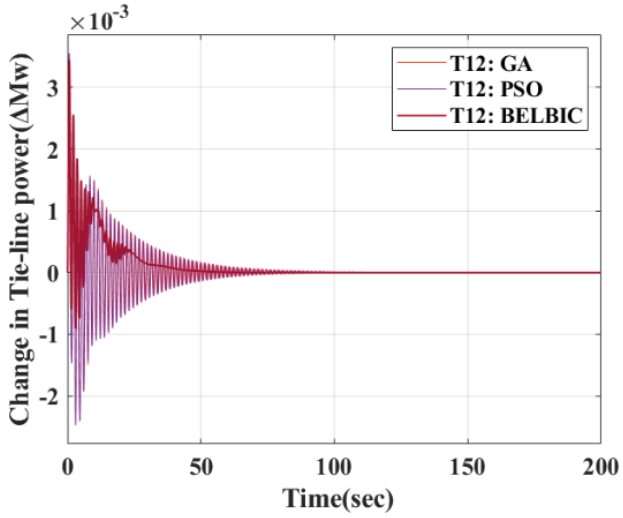

(iv)

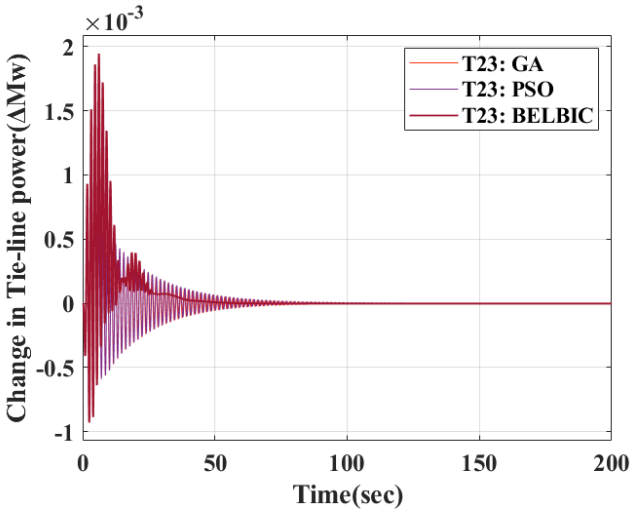

(v)

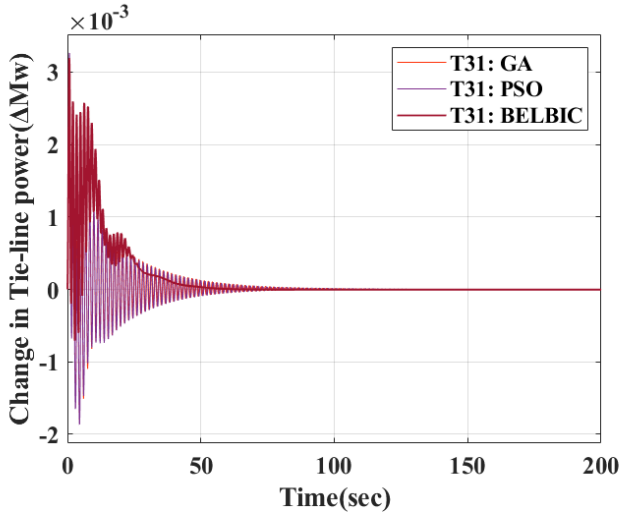

(vi)

Figure 9: Evaluation of 1% Change in load in AREA-1; (i) Variations in Area-1 frequency, (ii) Variations in Area-2 frequency, (iii) Variations in Area-3 frequency, and (iv) Variations in Area-1 and Area-2 Tie-Line Power (v) Variation in Area-2 and Area-3 Tie-Line Power (vi) Variation in the Tie-Line Power between Areas 1 and 3

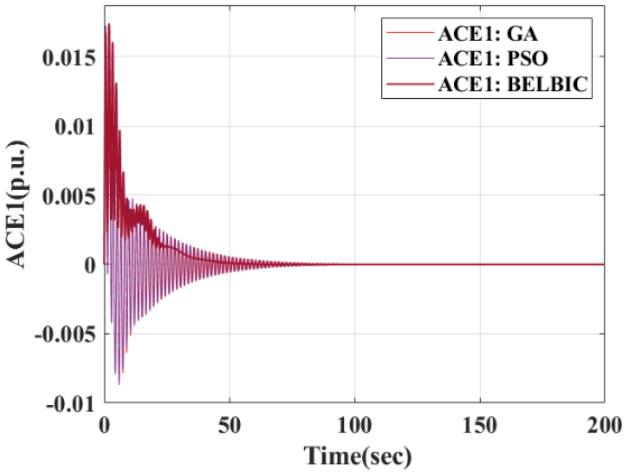

(vii)

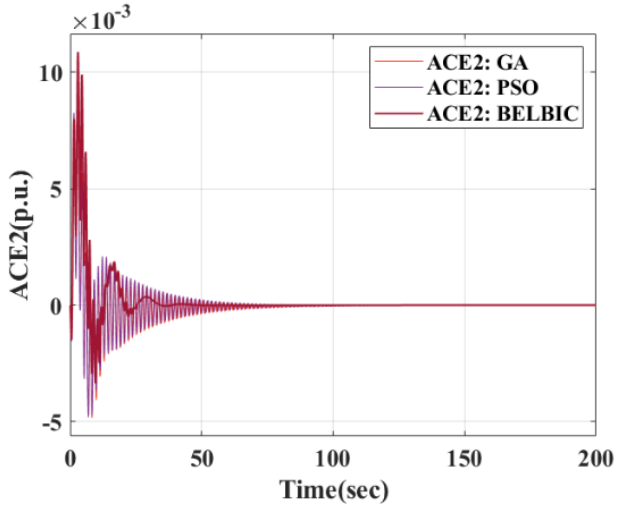

(viii)

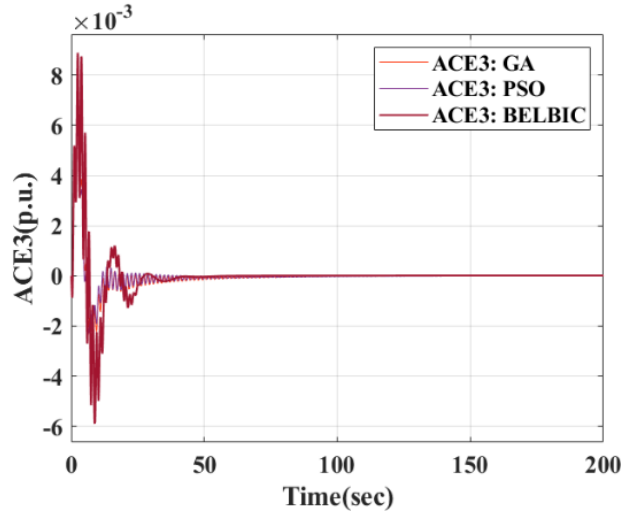

(ix)

Fig.10. The attainment of a 1% Change in load in AREA-1; Area Control Errors for Areas 1 through 3 are shown in (vii), (viii), and (ix) respectively.

Table:2 Steady State Error, Peak Under Shoot, Peak Over Shoot, and Settling Time Comparison Values for 1% Variation Load in Area-1

	STEADY STATE ERROR			PEAK OVER SHOOT			PEAK UNDER SHOOT			SETTLING TIME		
	GA	PSO	BELBI	GA	PSO	BELBI	GA	PSO	BELBI	GA	PSO	BELBI
ΔF_1	-0.000014	-0.000003	-0.00001	0.01241	0.01243	0.00586	-0.02091	-0.02061	-0.02591	120	90	33
ΔF_2	-0.000014	-0.000002	-0.00001	0.00823	0.00810	0.00615	-0.01738	-0.01692	-0.02197	110	90	33
ΔF_3	-0.000014	-0.000008	-0.00001	0.00648	0.00633	0.00764	-0.01434	-0.01396	-0.02258	100	100	33
ΔP_{tie1}	-0.000014	-0.000003	-0.00001	0.00353	0.00355	0.00344	-0.00234	-0.00244	-0.00084	145	120	50
ΔP_{tie2}	-0.000014	-0.000002	-0.00001	0.00095	0.00096	0.00194	-0.00084	-0.00084	-0.00091	115	120	50
ΔP_{tie3}	-0.000014	-0.000008	-0.00001	0.00324	0.00326	0.00319	-0.00018	-0.00186	-0.00064	115	100	55
ACE_1	-0.000014	-0.000003	-0.00001	0.01718	0.02478	0.01741	-0.00850	-0.00732	0.001125	135	100	55
ACE_2	-0.000014	-0.000002	-0.00001	0.00946	0.00929	0.01088	-0.00474	-0.00479	-0.00335	130	100	45
ACE_3	-0.000014	-0.000008	-0.00001	0.00601	0.00584	0.00889	-0.00259	-0.00258	-0.00588	115	120	42

4.2. SECTION-2

The proposed model is simulated in MATLAB/Simulink with the recommended controllers under a 0.02p.u. Fluctuation in load demand in Area-1. The frequency deviations, tie-line power, and area control error for the system dynamic reactions are shown in Figures 11 and 12. The BELBIC has better peak overshoot and peak undershoot characteristics than the PSO-PI and GA-PI tuned controllers, despite having a faster settling time. Finally, the developed controller outperforms the controller in terms of dynamic responsiveness. Although the frequency response of GA-PI and PSO-PI has superior peak overshoots and peak undershoots than the BELBIC controller, the latter is the quickest and exhibits high peak overshoots and undershoots for brief periods of time before quickly recovering to the steady state value. These peak values indicate a significant shift in the thermal steam turbine's mechanical power during peak over and under shoots, which will result in mechanical stress. Next, Table 3 presents the systems' dynamic responses. In comparison to GA-PI and PSO-PI, it was found that the BELBIC controller has a shorter settling time. This suggests that compared to other controllers, this one has a superior dynamic reaction.

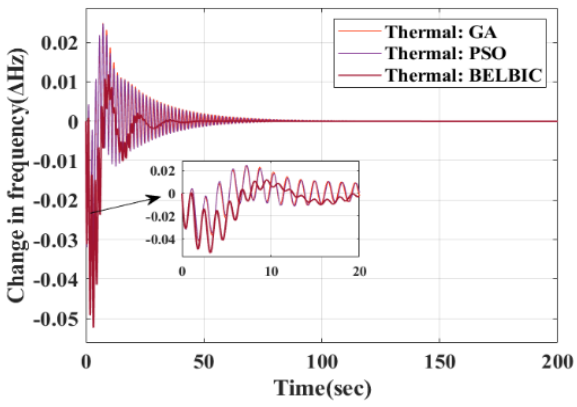

(i)

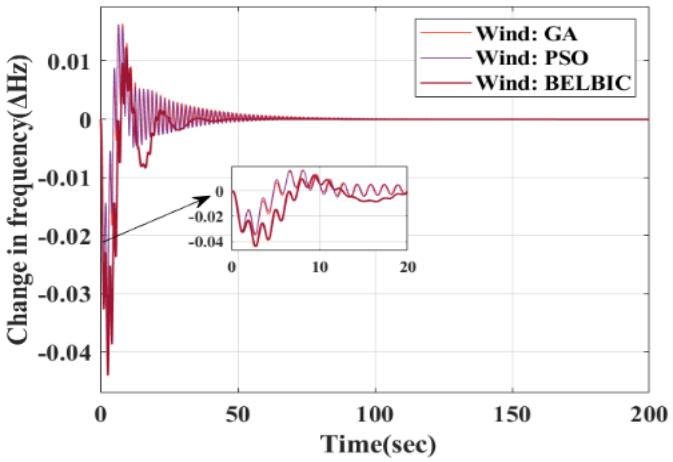

(ii)

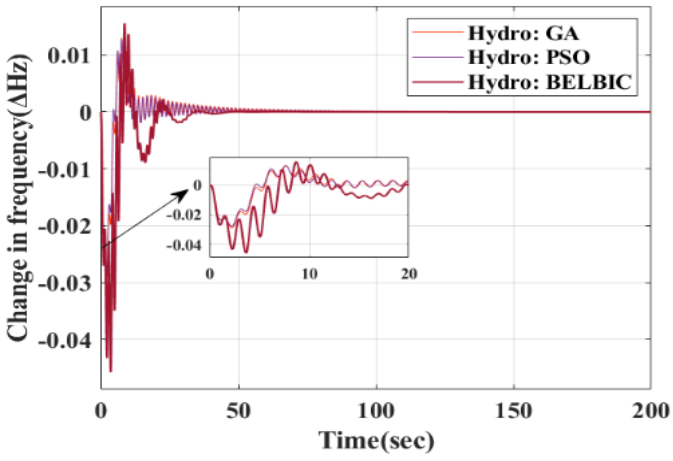

(iii)

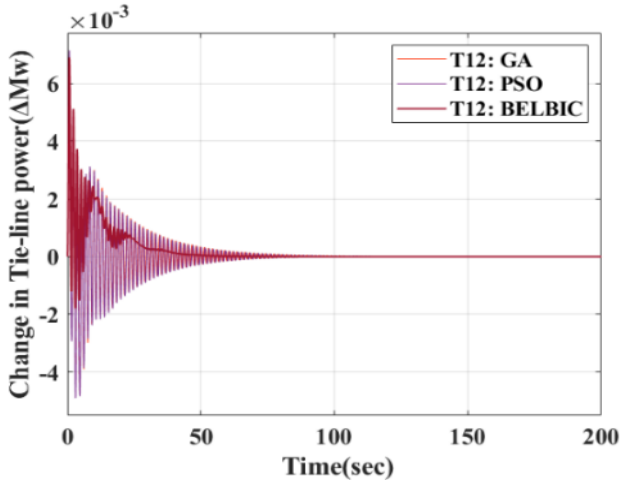

(iv)

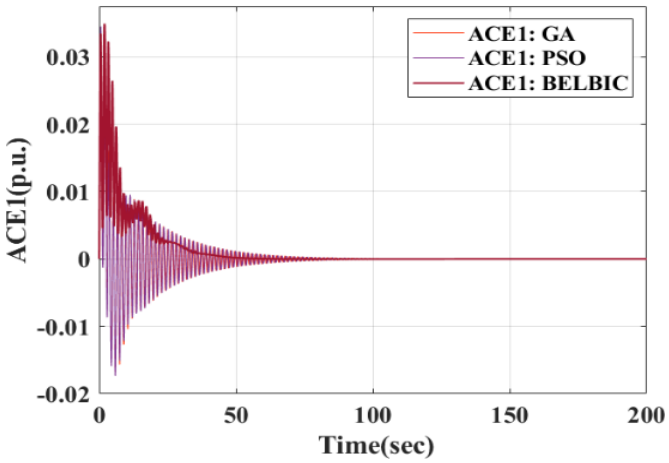

(vii)

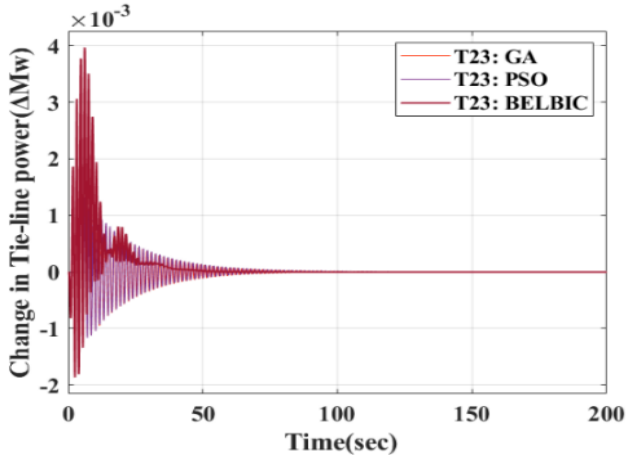

(v)

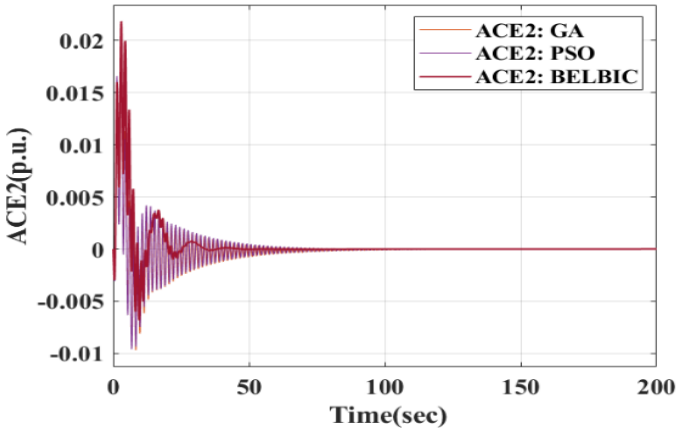

(viii)

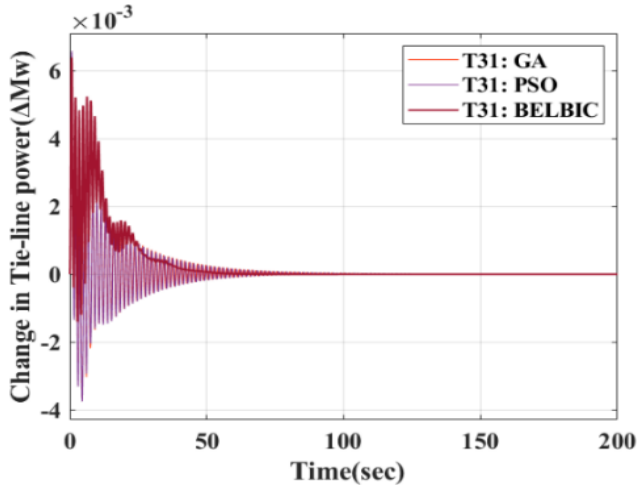

(vi)

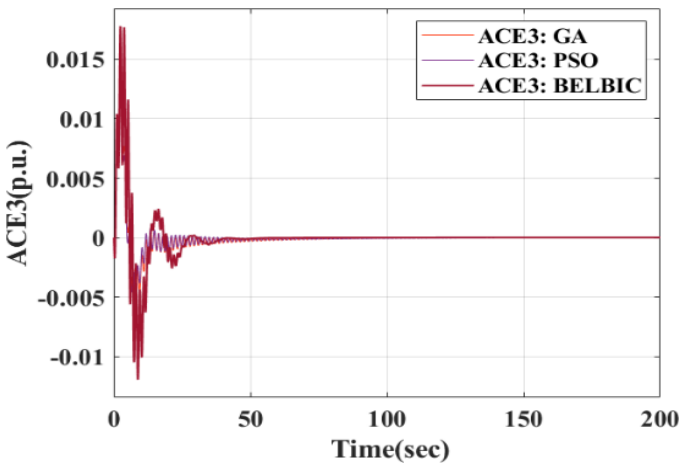

(ix)

Figure 11: Evaluation of 1% Change in load in AREA-1; (i) Variations in Area-1 frequency, (ii) Variations in Area-2 frequency, (iii) Variations in Area-3 frequency, and (iv) Variations in Area-1 and Area-2 Tie-Line Power (v) Variation in Area-2 and Area-3 Tie-Line Power (vi) Variation in the Tie-Line Power between Areas 1 and 3

Fig.12. The attainment of a 1% Change in load in AREA-1; Area Control Errors for Areas 1 through 3 are shown in (vii), (viii), and (ix) respectively.

Table:3 Steady State Error, Peak Under Shoot, Peak Over Shoot, and Settling Time Comparison Values for 1% Variation Load in Area-1

	STEADY STATE ERROR			PEAK OVER SHOOT			PEAK UNDER SHOOT			SETTLING TIME		
	GA	PSO	BELBI	GA	PSO	BELBI	GA	PSO	BELBI	GA	PSO	BELBI
ΔF_1	-0.000028	-0.000006	-0.000032	0.02487	0.02471	0.01185	-0.04201	-0.04135	-0.052305	120	90	33
ΔF_2	-0.000028	-0.000054	-0.000032	0.01639	0.01629	0.01238	-0.03480	-0.03370	-0.044216	110	90	33
ΔF_3	-0.000029	-0.000057	-0.000032	0.01300	0.01266	0.01553	-0.02867	-0.02804	-0.045658	100	100	33
ΔP_{tie1}	-0.000028	-0.000006	-0.000032	0.00719	0.00715	0.00690	-0.004715	-0.00491	-0.001795	145	120	50
ΔP_{tie2}	-0.000028	-0.000054	-0.000032	0.00188	0.00193	0.00396	-0.001669	-0.00413	-0.001871	115	120	50
ΔP_{tie3}	-0.000029	-0.000057	-0.000032	0.00654	0.00657	0.01553	-0.003669	-0.00376	-0.045746	115	100	55
ACE_1	-0.000028	-0.000006	-0.000032	0.03431	0.03450	0.03492	-0.01700	-0.01723	0.001125	135	100	50
ACE_2	-0.000028	-0.000054	-0.000032	0.01891	0.01855	0.02184	-0.009470	-0.00961	-0.006800	130	100	45
ACE_3	-0.000029	-0.000057	-0.000032	0.01204	0.01171	0.01777	-0.005192	-0.00518	-0.011911	115	120	42

4.3. SECTION-3

The suggested model is simulated in MATLAB/Simulink under a 0.05 p.u. change in load demand in Area-1, confirming the BELBIC's robustness once more. The frequency deviations, tie-line power, and area control error for the system dynamic reactions are shown in Figures 13 and 14. The BELBIC has better peak overshoot and peak undershoot characteristics than the PSO-PI and GA- PI tuned controllers, despite having a faster settling time. Finally, the developed controller outperforms the controller in terms of dynamic responsiveness. The BELBIC has better peak overshoot and peak undershoot characteristics than the PSO-PI and GA-PI tuned controllers, despite having a faster settling time. Next, Table 3 presents the systems' dynamic responses. Finally, the developed controller outperforms the controller in terms of dynamic responsiveness.

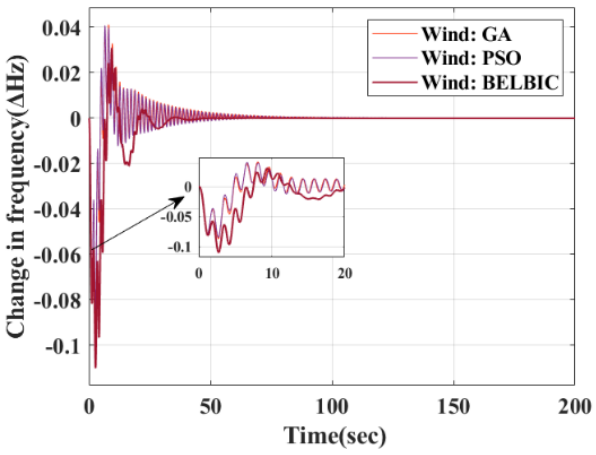

(ii)

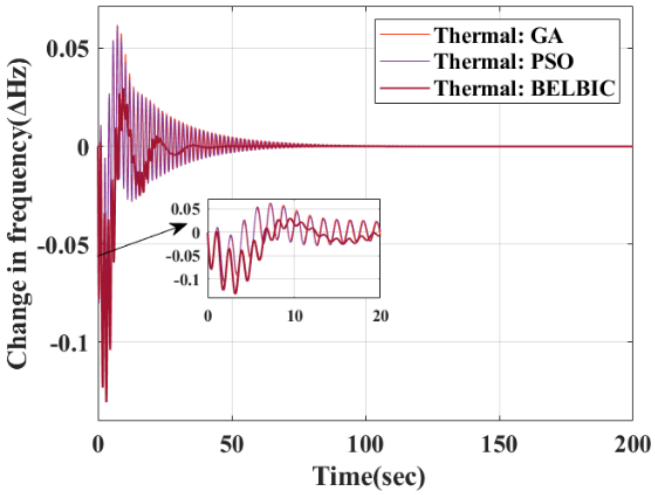

(i)

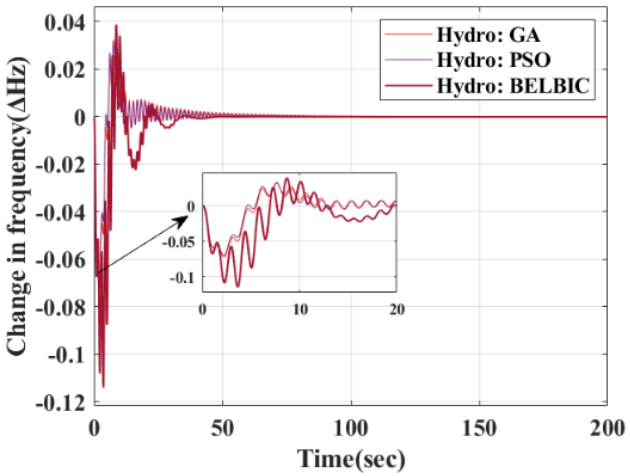

(iii)

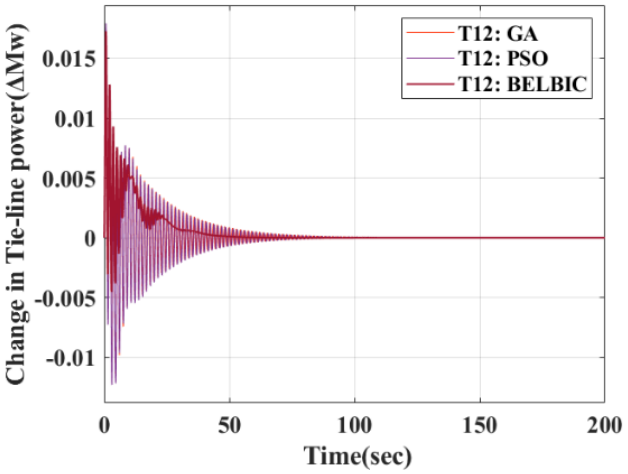

(iv)

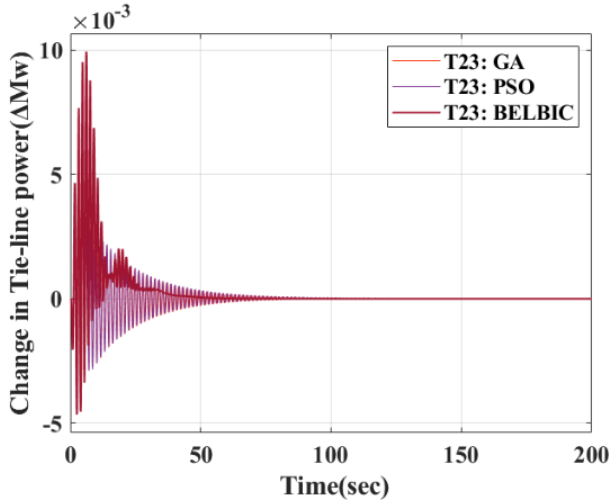

(v)

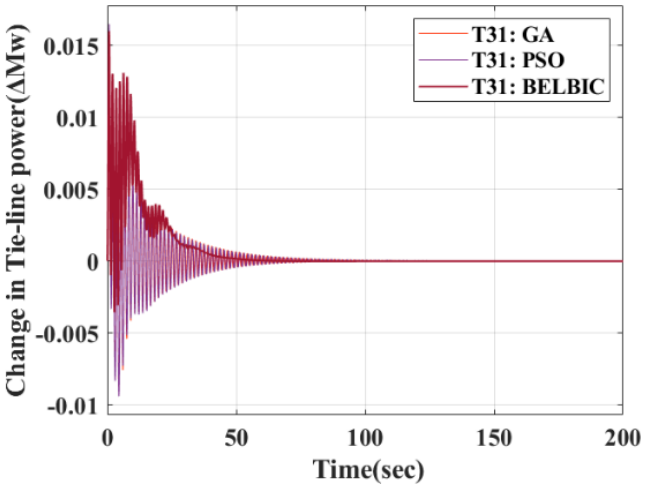

(vi)

Figure 13: Evaluation of 1% Change in load in AREA-1; (i) Variations in Area-1 frequency, (ii) Variations in Area-2 frequency, (iii) Variations in Area-3 frequency, and (iv) Variations in Area-1 and Area-2 Tie-Line Power (v) Variation in Area-2 and Area-3 Tie-Line Power (vi) Variation in the Tie-Line Power between Areas 1 and 3

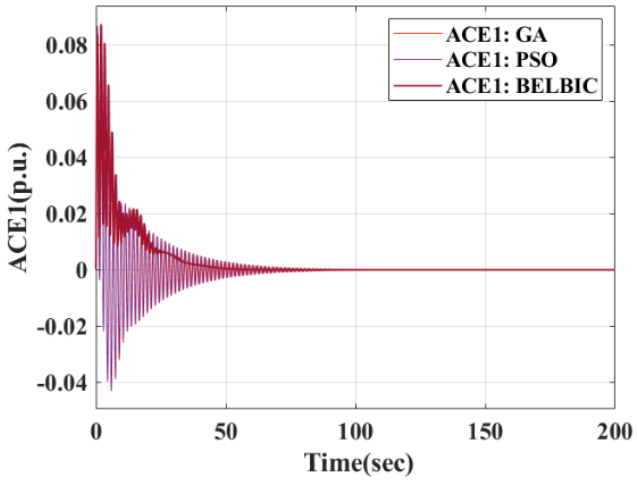

(vii)

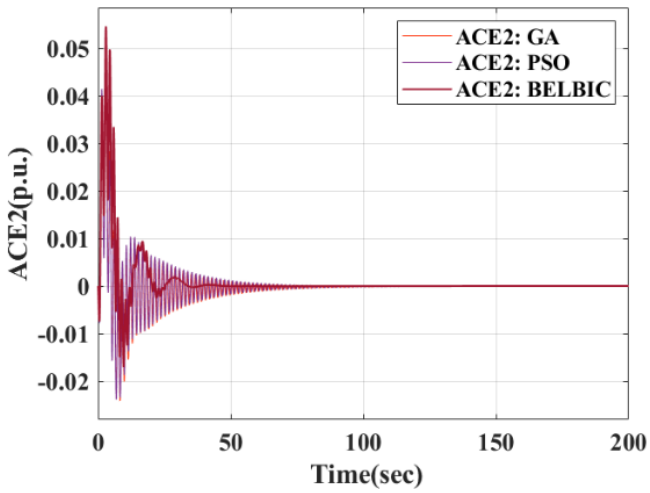

(viii)

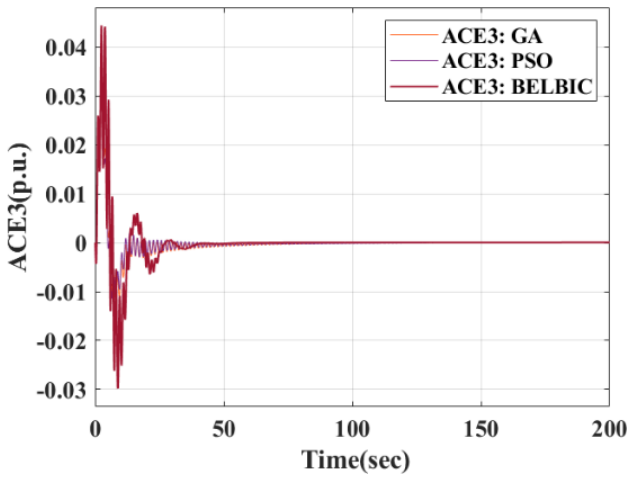

(ix)

Fig.14. The attainment of a 1% Change in load in AREA-1; Area Control Errors for Areas 1 through 3 are shown in (vii), (viii), and (ix) respectively.

Table:4 Steady State Error, Peak Under Shoot, Peak Over Shoot, and Settling Time Comparison Values for 1% Variation Load in Area-1

	STEADY STATE ERROR			PEAK OVER SHOOT			PEAK UNDER SHOOT			SETTLING TIME		
	GA	PSO	BELBI	GA	PSO	BELBI	GA	PSO	BELBI	GA	PSO	BELBI
ΔF_1	-0.000072	-0.000015	-0.000081	0.06200	0.06162	0.02961	-0.01507	-0.10405	-0.13083	120	90	33
ΔF_2	-0.000072	-0.000013	-0.000081	0.04118	0.04080	0.03094	-0.08724	-0.08437	-0.011019	110	90	33
ΔF_3	-0.000072	-0.000014	-0.000082	0.03249	0.03160	0.03880	-0.07159	-0.06988	-0.11426	100	100	33
ΔP_{tie1}	-0.000072	-0.000015	-0.000081	0.01783	0.01792	0.01725	-.0.01190	-0.01223	-0.004509	145	120	50
ΔP_{tie2}	-0.000072	-0.000013	-0.000081	0.00476	0.00486	0.00992	-0.00429	-0.00437	-0.004677	115	120	50
ΔP_{tie3}	-0.000072	-0.000014	-0.000082	0.01641	0.01649	0.01598	-0.00919	-0.00924	-0.009840	115	100	55
ACE_1	-0.000072	-0.000015	-0.000081	0.08623	0.08668	0.08737	-0.04221	-0.04289	0.001125	135	100	50
ACE_2	-0.000072	-0.000013	-0.000081	0.04710	0.04614	0.05463	-0.02373	-0.02367	-0.0172	130	100	45
ACE_3	-0.000072	-0.000014	-0.000082	0.03012	0.02930	0.04439	-0.01300	-0.01305	-0.029768	115	120	42

5. Conclusion And Future Scope

In summary, this research presented a recently studied Brain Emotional Learning Based Intelligent Controller (BELBIC) for power systems load frequency regulation. Under load disturbances in three different locations, the performance of the planned BELBIC was assessed and contrasted with that of the PSO-PI and GA-PI tuned controllers. To evaluate the controller's resilience to changes in load and parameter fluctuations, simulation simulations were carried out using MATLAB. The findings show that, especially when system characteristics and load levels fluctuate, the suggested BELBIC dynamically responds better than the PSO-PI and GA-PI tuned controller. The results confirm how well the BELBIC works to solve load frequency control issues in power networks. Its resilience and appropriateness for real-world applications are demonstrated by its capacity to adjust to changes in parameters and manage higher loads. These findings demonstrate how computational intelligence methods, such the BELBIC, can improve power system control and guarantee steady, dependable operation. Other facets of the BELBIC and its application in actual power systems can be investigated through more study and testing.

6. References

[1] N.E.Y. Kouba, M. Menaa, M. Hasni, M. Boudour, Load Frequency Control in multi-area power system based on Fuzzy Logic-PID Controller, in 2015 IEEE International Conference on Smart Energy Grid Engineering (SEGE), Oshawa, ON, Canada, 2015.

[2] Feleke, S., Satish, R., Salkuti, S.R., Abdelaziz, A.Y. Load Frequency Control in Two-Area Interconnected Systems Using DE-PID and PSO-PID. In: Salkuti, S.R., Ray, P., Singh, A.R. (eds) Power Quality in Microgrids: Issues, Challenges and Mitigation Techniques. Lecture Notes in Electrical Engineering, vol 1039. Springer, Singapore.2023

[3] Kodakkal. A., Veramalla, R., Salkuti, S.R. Optimized Control of an Isolated Wind Energy Conversion System. In: Salkuti, S.R. (eds) Energy and Environmental Aspects of Emerging Technologies for Smart Grid. Green Energy and Technology. Springer, Cham.2024.

[4] Asma Aziz, Aman Than Oo, Alex Stojcevski," Analysis of frequency sensitive wind plant penetration effect on load frequency control of hybrid power system", International Journal of Electrical Power & Energy Systems, vol.99, pp.603-617, July 2018.

[5] Sarker, Md, Hasan, Kamrul. “Load Frequency Control in Power System”. 10. 23-30. 2016.

[6] Prabha S Kundur and Om P Malik. Power system stability and control. McGraw-Hill Education, 2022.

[7] Mohammad Amir, Kavita Singh,Chapter 16 - Frequency regulation strategies in renewable energy-dominated power systems: Issues, challenges, innovations, and future trends, Editor(s): Sandeep Dhundhara, Yogendra Arya, Ramesh C. Bansal, Advanced Frequency Regulation Strategies in Renewable-Dominated Power Systems, Academic Press, 2024, Pages 367-381, ISBN 9780323950541,

[8] Z. A. Obaid, L. M. Cipcigan, L. Abrahim, and M. T. Muhssin, “Frequency control of future power systems: reviewing and evaluating challenges and new control methods,” J. Mod. Power Syst. Clean Energy, 2019, vol. 7, no. 1, pp. 9–25. [11]

[9] Mohammed Wadi, Abdulfetah Shobole, Wisam Elmasry, Ismail Kucuk, Load frequency control in smart grids: A review of recent developments, Renewable and Sustainable Energy Reviews, Volume 189, Part A, 2024, 114013, ISSN 1364-0321,

[10] D. H. Tungadio and Y. Sun, “Load frequency controllers considering renewable energy integration in power system,” Energy Reports, 2019, vol. 5, pp. 436–453.

[11] harma, Navdeep Singh,Load frequency control of connected multi-area multi-source power systems using energy storage and lyrebird optimization algorithm tuned PID controller, Journal of Energy Storage, Volume 100, Part B, 2024, 113609, ISSN 2352-152X,

[12] Abdul Latif, S.M. Suhail Hussain, Dulal Chandra Das, Taha Selim Ustun, “State-of-the-art of controllers and soft computing techniques for regulated load frequency management of single/multi-area traditional and renewable energy-based power systems, Applied Energy, Volume 266, 2020, 114858, ISSN 0306-2619

[13] Tshinavhe, Ntanganedzeni Ratshitanga, Mukovhe, Tsheme, Nomzamo. Review of Adaptive Load Frequency Control Strategies for Improving Wind Power Plant Integration, 2024, pp 1-6.

[14] Irfan Ahmed Khan, Hazlie Mukhlis, Nurulafiqah Nadzirah Mansor, Hazlee Azil Illias, Lilik Jamilatul Awalin, Li Wang, “New trends and future directions in load frequency control and flexible power system:

A comprehensive review", Alexandria Engineering Journal, Volume 71, 2023, Pages 263-308, ISSN 1110-0168.

[15] M.H. Soliman, H.E.A. Talaat, M.A. Attia, "Power system frequency control enhancement by optimization of wind energy control system", Ain Shams Eng. J. 12 (4) (Dec. 2021) 3711– 3723,

[16] Asghar R, Riganti Fulginei F, Wadood H, Saeed S. A Review of Load Frequency Control Schemes Deployed for Wind-Integrated Power Systems. Sustainability. 2023; 15(10):8380.

[17] K. Kaur and Y. Kumar, "Swarm Intelligence and its applications towards Various Computing: A Systematic Review," Proc. Int. Conf. Intell. Eng. Manag. ICIEM 2020, pp. 57–62, 2020,

[18] Namrata, K., Kumar, N., Sekhar, C., Gupta, R.P., Salkuti, S.R. Modeling and Sizing of the Hybrid Renewable System Opting Genetic Algorithm. In: Salkuti, S.R., Ray, P., Singh, A.R. (eds) Power Quality in Microgrids: Issues, Challenges and Mitigation Techniques. Lecture Notes in Electrical Engineering, vol 1039. Springer, Singapore. 2023

[19] J. Shankar Mallesham, G & Surrender Reddy. S. Optimal Tuning of PI Controller for Automatic Generation Control in Multi-Area Power Systems Using PSO for Enhanced Load Frequency Control. *Journal of Electrical Systems*, *20*(3s), 6983-6998 (2024).

[20] M. M. Sati, D. Kumar, A. Singh, M. Raparthi, F. Y. Alghayadh and M. Soni, "Two-Area Power System with Automatic Generation Control Utilizing PID Control, FOPID, Particle Swarm Optimization, and Genetic Algorithms," 2024 Fourth International Conference on Advances in Electrical, Computing, Communication and Sustainable Technologies (ICAECT), Bhilai, India, 2024, pp. 1-6,

[21] Ram Babu, N., Bhagat, S.K., Saikia, L.C. et al. A Comprehensive Review of Recent Strategies on Automatic Generation Control/Load Frequency Control in Power Systems. Arch Computat Methods Eng 30, 543–572 (2023).

[22] H. K. Shaker, H. E. Zoghbv, M. E. Bahgat and A. M. Abdel-Ghany, "Load Frequency Control for An Interconnected Multi Areas Power System Based on optimal Control Techniques," 2020 12th International Conference on Electrical Engineering (ICEENG), Cairo, Egypt, 2020, pp. 62-67,

[23] Gachhadar A, Maharjan RK, Shrestha S, Adhikari NB, Qamar F, Kazmi SHA, Nguyen QN. Power Optimization in Multi-Tier Heterogeneous Networks Using Genetic Algorithm. Electronics. 2023; 12(8):1795.

[24] Ehsan Lotfi and Abbas Ali Rezaee, "Generalized BELBIC", A.A. Neural Comput & Applic, 2018, pp.1-16. IWOBI 2019 IEEE International Work Conference on Bioinspired Intelligence

[25] Caro Lucas, Danial Shahmirzadi, and Nima Sheikholeslami. Introducing belbic: brain emotional learning based intelligent controller. Intelligent Automation & Soft Computing, 10(1):11–21,

[26] D. Valencia and D. Kim, "Trajectory Tracking Control for Multiple Quadrotors Based on a Neurobiological-Inspired System," 2019 Third IEEE International Conference on Robotic Computing (IRC), Naples, Italy, 2019, pp. 465-470,

[27] D. L. N. Sravani and K. H. Phani Shree, "Artificial Neural Network Controller for Doubly Fed Induction Generator-Based Wind Energy Conversion System," 2024 IEEE 4th International Conference on Sustainable Energy and Future Electric Transportation (SEFET), Hyderabad, India, 2024, pp. 1-6,

[28] M. S. O. Yeganeh, A. Oshnoei, N. Mijatovic, T. Dragicevic and F. Blaabjerg, "Intelligent Secondary Control of Islanded AC Microgrids: A Brain Emotional Learning-Based Approach," in IEEE Transactions on Industrial Electronics, vol. 70, no. 7, pp. 6711-6723, July 2023

[29] M. R. Khalghani, and N. Vafamand, "A self-tuning load frequency control strategy for microgrids: Human brain emotional learning," Int. J. Electr. Power Energy Syst., Vol. 75, pp. 311–319, Feb. 2016.

[30] M. M. Zirkohi, "An Efficient optimal fractional emotional intelligent controller for an AVR system in power systems," J. Artifcl. Intel. Data. Min, Vol. 7, pp. 193–202, Mar. 2019.

[31] A Khodabakhshian and R Hooshmand. A new pid controller design for automatic generation control of hydro power systems. International Journal of Electrical Power & Energy Systems, 32(5):375–382, 2010.

[32] Gayadhar Panda, Sidhartha Panda, and Cemal Ardil. Automatic generation control of interconnected power system with generation rate constraints by hybrid neuro fuzzy approach. International journal of electrical power and energy systems engineering, 2(1):13–18, 2009.

[33] Xiangjie Liu, Xiaolei Zhan, and Dianwei Qian. Load frequency control considering generation rate constraints. In 2010 8th World Congress on Intelligent Control and Automation, pages 1398–1401. IEEE, 2010.

[34] Le-Ren Chang-Chien, Wei-Ting Lin, and Yao-Ching Yin. Enhancing frequency response control by dfigs in the high wind penetrated power systems. IEEE transactions on power systems, 26(2):710–718, 2010.

[35] Naresh Kumari and A N Jha. Particle swarm optimization and gradient descent methods for optimization of pi controller for agc of multiarea thermal-wind-hydro power plants. In 2013 UK Sim 15th International Conference on Computer Modelling and Simulation, pages 536– 541,

[36] Nicolaos et. all Munteanu, Iulian. Optimal Control of Wind Energy Systems, Towards a Global Approach. 01 2008

[37] Gachhadar A, Maharjan RK, Shrestha S, Adhikari NB, Qamar F, Kazmi SHA, Nguyen QN. Power Optimization in Multi-Tier Heterogeneous Networks Using GA. Electronics. 2023; 12(8):1795.

[38] A. Gupta, R. P. Saini and M. P. Sharma, "Modelling of the hybrid energy system-Part I: Problem formulation and model development," Renewable Energy, vol. 36, no. 2, pp. 459–465, 2011.

[39] Xin Xu, Han-gen He, and Dewen Hu. Efficient reinforcement learning using recursive least-squares methods. Journal of Artificial Intelligence Research, 16:259–292, 2002.

[40] M Fatourechi, C Lucas, and A Khaki Sedigh. Reducing control effort by means of emotional learning. In Proceedings of 19th Iranian conference on electrical engineering, volume 41, pages 1–41, 2001.

[41] Jan Moren and Christian Balkenius. A computational model of emotional learning in the amygdala. 01 2000.

[42] J. Shankar G. Mallesham "Automatic generation control of multi area power systems using BELBIC" in 4th Electric Power and Renewable Energy Conference (EPREC-2023) Springer 2023.

[43] Arpit Jain, "Computational Modeling of the Brain Limbic System and Its Application in Control Engineering", Master dissertation, Electrical and Instrumentation Engineering Department, Thapar University Patiala, 2009

[44] Moren J., "Emotion and Learning - A Computational Model of the Amygdala", PhD dissertation, Department of Cognitive Science, Lund University, 2002

[45] Moren J. and Balkenius C., "A Computational Model of Emotional Learning in the Amygdala", in Proceedings of the 6th International Conference on the Simulation of Adaptive Behavior, Vol.6, 2000, pp.383-391

[46] A. A. El-Gawad, A. N. Elden, M. E. Bahgat and A. M. Abdel Ghany, "BELBIC Load Frequency Controller Design for a Hydro-Thermal Power System," 2019 21st International Middle East Power Systems Conference (MEPCON), Cairo, Egypt, 2019, pp. 809-814,